Designing small molecules as ternary energy-cascade additives for polymer:fullerene solar cell blends

Angela Punzi,[†#] Alessandra Operamolla,[†#] Omar Hassan Omar,[I] Francesca Brunetti,[□] Alberto D. Scaccabarozzi,[‡,°] Gianluca M. Farinola,[*†] and Natalie Stingelin[*,⊥§]

[†] Dipartimento di Chimica, Università degli Studi di Bari Aldo Moro, Via Orabona 4, I-70126 Bari, Italy

[I] CNR-ICCOM Istituto di Chimica dei Composti Organometallici, Via Orabona 4, I-70126 Bari, Italy

[□] Centre for Hybrid and Organic Solar Energy (CHOSE), Dipartimento di Ingegneria Elettronica, Università degli Studi di Roma "Tor Vergata", via del Politecnico 1, 00133 Roma, Italy

[‡] Department of Materials and Centre of Plastic Electronics, Imperial College London, London SW7 2AZ, UK.

[⊥] School of Materials Science and Engineering and School of Chemical and Biomolecular Engineering, Georgia Institute of Technology, 311 Ferst Drive, Atlanta, GA 30332, United States

[§] Laboratoire de Chimie des Polymeres Organiques – LCPO, UMR5629 Université de Bordeaux, Allee Geoffroy Saint Hilaire, Batiment BB CS50023, 33615 Pessac Cedex, France

KEYWORDS. Polymer solar cells; thiols; bulk-heterojunction; light harvesting; organic photovoltaics.

ABSTRACT: Ternary blends comprising an 'energy-cascade former' in addition to the donor and the acceptor materials increasingly attract attention in the organic solar cell area as they seem to provide a tool to positively manipulate the open-circuit voltage of bulk-heterojunction devices. By comparing two additives that have similar HOMO/LUMO levels and that can be expected to lead to an energy cascade in ternaries with the prototypical P3HT:$PC_{60}BM$ system, we demonstrate here that the compatibility of the additive with, in this specific case, the fullerene can be tailored by peripheral chemical functionalization and plays a critical role. A compromise needs to be found between good mixing (favoring energy cascade formation) and phase separation (supporting charge extraction) that affect the open-circuit voltage in as important fashion as their electronic features, providing critical insights for future materials design activities.

The active layer of bulk-heterojunction (BHJ) solar cells is generally based on a blend of two organic semiconductors (small molecules or polymers) with different electron affinities and forming a bi-continuous interpenetrating network, often with a highly complex phase morphology.[1] One component acts as the electron-donating material (donor) and the other as the electron-accepting material (acceptor). While efficiencies of more than 12 % have now been reported,[2] key issues that remain challenging to solve are: *i*) the often demanding synthesis of the donor and/or acceptor rendering scale up difficult;[3] *ii*) the limited, intrinsic light absorption of many current donor:acceptor systems, as well as *iii*) the non-optimal positioning of the frontier energy levels of the donor and the acceptor. Indeed, a large energetic offset between the lowest unoccupied molecular orbitals (LUMO) of many donors compared to those of the acceptors can lead to a significant energy loss in the photoinduced electron transfer from the donor to the acceptor material, reducing the output power of the solar cells. *Vice versa*, too small differences in energy levels often limit the driving force for exciton dissociation. Many of these issues, as well as non-radiative recombination losses, directly influence the open-circuit voltage, V_{OC}.[4] As a consequence, the design of donor and acceptor materials can be intricate.

One promising strategy to address these challenges is to employ ternary BHJ blends.[5] Ternary solar cells offer the advantage of maintaining straightforward processing conditions, being based on a single active layer, with respect to more complex device architectures. Conversely, they pose the challenge to control much more complex three components electronic and morphological interactions. In the case of the prototypical BHJ blend of poly(3-hexylthiophene) (P3HT) and the fullerene derivative [6,6]-phenyl-C_{61} butyric acid methyl ester ($PC_{60}BM$), low bandgap polymers,[6] small conjugated molecules[7] and nanoparticles[8] have already been used -with varying success-as ternary component to enhance light harvesting and/or generate an energy level cascade, tackling point *ii*) ad *iii*). However, clear structure/processing/property interrelations and insights on how the additives need to be structurally integrated in the complex BHJ architecture remain elusive.

In order to establish the much needed structural picture and how it relates to the electronic landscape of such donor:acceptor blends, we employed here two molecular additives featuring the same conjugated framework. One of them possesses thioacyl peripheral chemical functionalization. This allows us to tailor its miscibility with the fullerene component of the ternary blend. The two molecular additives display a donor-acceptor-donor (D-A-D) architecture comprising an electron-poor benzo[*c*][1,2,5]thiadiazole-central unit, symmetrically coupled in its 4,7-positions with two electron-rich bis-thiophene segments (**Fig. 1a**), *i.e.* 4,7-bis(5'-hexyl-2,2'-bithiophen-5-yl)benzo[*c*][1,2,5]thiadiazole (**4T1B**)[9-13] and S,S'-6,6'-[5',5"-(benzo[*c*][1,2,5]thiadiazole-4,7-diyl)bis(2,2'-bithiophene-5',5-diyl)]bis(hexane-6,1-diyl)diethanethioate (**4T1BSAc**). The synthesis of these ternary components is simple and straightforward (see the SI for details). In addition, these two additives seemed ideal for our purpose as our past studies[14] have indicated that: (*i*) **4T1B** and **4T1BSAc** display nearly identical energy levels (estimated from electrochemical and optical measurements: see SI, Figs. S11-14; data are summarized in **Table 1**), that are in between those of P3HT and $PC_{60}BM$ and, thus, should lead to an energy-level cascade that can lead to efficient charge separation (**Fig. 1b**/inset); *(ii)* they display meagre attitude for resonant energy transfer in the ternary blend, due to the poor overlap between the solid state emission from P3HT and additives absorption profile

Table 1. Comparison of optical, electronics and thermal data obtained for **4T1B** and **4T1BSAc**.

Compound	$\lambda_{max,abs}$ [nm][a]	$\lambda_{max,PL}$ [nm][a]	$E_{g,opt}$ [eV][b]	E_{HOMO} [eV][c]	E_{LUMO} [eV][c]	$E_{g,ec}$ [eV][d]	μ [$cm^2V^{-1}s^{-1}$][e]	Transition temperatures [°C][f]
4T1BSAc	364, 518	658	2.05	-5.46	-3.38	2.08	$2.5\cdot10^{-5}$	121, 143, 172, 179
4T1B	363, 518	652	2.05	-5.50	-3.42	2.08	$4.6\cdot10^{-5}$	120, 173, 200, 208

[*](a) Measured in 10^{-4} M $CHCl_3$ solution. (b) Optical band gap estimated as $E_g = 1240/\lambda_{onset}$. (c) HOMO and LUMO levels were estimated with the empirical equations: HOMO = -e(E_{ox} + 5.1) V and LUMO = -e(E_{red} + 5.1) V.[19] (d) Electrochemical band gap. (e) Hole mobility in bottom gate-bottom contact OFETs measured in the saturation regime; (f) Thermal transitions deduced from DSC.

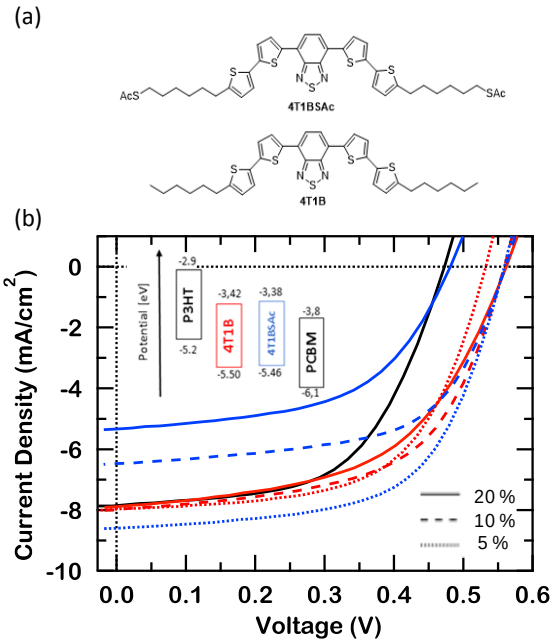

Figure 1. a) Chemical structure of **4T1BSAc** and **4T1B**. b) Current density of best performing devices versus applied bias for different loading percentages under illumination: 0%, 5%, 10%, 20% wt of **4T1BSAc** and **4T1B**. The inset shows the energy levels of **4T1B**, **4T1BSAc**, P3HT and $PC_{60}BM$. HOMO and LUMO levels of **4T1B** and **4T1BSAc** were estimated from cyclic voltammograms recorded on a 1.0 mM solution on a Pt working electrode in 0.1M n-Bu_4NPF_6 in anhydrous CH_2Cl_2 at $0.2Vs^{-1}$ and room temperature (see Fig. S11).

and between additives solid state emission and P3HT aggregation bands absorption (see SI, Figure S13); (*iii*) they feature very similar, albeit modest charge transport properties, as measured in non-optimized bottom-gate/bottom-contact solution-processed field-effect transistors (**Table 1** and SI, Fig. S16), with hole mobilities of $4.6\cdot10^{-5}$ and $2.5\cdot10^{-5}$ $cm^2(Vs)^{-1}$ in the saturation regime for **4T1B** and **4T1BSAc**, respectively; (*iv*) they follow a comparable, complex thermal phase behavior in the neat form, as judged from differential scanning calorimetry (DSC) measurements, with a liquid crystalline behavior observed in both cases, resulting in distinct, multiple endotherms at 120, 173, 200, 208 °C for **4T1B** and at 121, 143, 172, 179 °C for **4T1BSAc** (Table 1; more details provided in SI, Fig. S15) and melting enthalpies of 22.104 mJ mg^{-1} at 173°C for **4T1B** and 20.602 mJ mg^{-1} at 143°C for **4T1BSAc**; and *(v)* they are expected to display a different solid-state structure formation in BHJ blends due to the thiol functionalization in **4T1BSAc** which likely leads to a different phase behavior with the OPV blend compared to the unsubstituted **4T1B**. Thiol esters are stable functional groups[15] and are structurally related to alkylthiols, that are select-give solvents for $PC_{60}BM$, the positive effect of which on the phase morphology and performances of P3HT: $PC_{60}BM$ blends has been demonstrated.[16] Therefore, here the chemical functionalization of the ternary molecule with a functional group able to modulate the miscibility property of a small donor material is proposed as new strategy to finely control a ternary blend morphology. This chemical approach has the potentiality to be of general use, and alternative to other case-specific examples such as the use of materials with complex molecular structure and demanding synthesis[17,18] as driving force for generation of an ideal cascade morphology in which the third component has to be located at the P3HT/PCBM heterojunction.

In order to elucidate the effect of the two potential energy-cascade formers in ternary BHJ devices, we prepared P3HT:$PC_{60}BM$ solar cells containing different fractions of **4T1BSAc** or **4T1B** (5, 10, 20 wt% with respect to P3HT), using a standard device geometry (ITO/PEDOT:PSS/P3HT: $PC_{60}BM$/ Li/Al). Reference devices without 'additives' were prepared for comparison. The corresponding *J-V* characteristics are shown in the Fig. 1b, while their device parameters are summarized in the Table 2. Reassuringly, and as expected from the energy levels of **4T1BSAc** and **4T1B**, we observe an increase in V_{OC} to the maximum value of 0.56V for the majority of the ternary blend devices, in agreement with the expected picture that the *Voc* is driven by a ternary cascaded mechanism[5c,20] and pinned by the electronic structure of the two additives (featuring the same HOMO and LUMO levels as previously demonstrated), rather than by other mechanisms like an intimate mixture of the donor polymer with the additive, acting as an organic alloy of donors, that would rather induce *Voc* linear variations with the additive:P3HT weight ratio.[21] Given the expected ternary cascade effect, for the compositions analyzed blends with **4T1B** display an increase of the V_{OC} from 0.47 V to 0.56 V, while *Jsc* remained essentially identical compared to the reference device comprising no additive. A notably different behavior is found for systems comprising **4T1BSAc**. An increase in V_{OC} is recorded only for ternaries comprising a relatively small fraction of this additive (5 and 10 wt% with respect to the P3HT content). At higher content both V_{OC} and J_{SC} drastically decrease. However, compared to the ternaries comprising **4T1B**, it is striking to observe that small amounts of **4T1BSAc** seem to not only increase V_{OC} but also

Table 2. Device parameters measured for P3HT:$PC_{60}BM$ (1:0.8 w/w) solar cells comprising different weight fractions of **4T1BSAc** and **4T1B**. Statistical variations of *J*sc, *V*oc, FF and PCE are listed in the SI, Figs. S17-18.

Additive	J_{sc} [$mA\cdot cm^{-2}$]	V_{oc} [V]	FF	$PCE_{max/av}$ (%)
No additive	7.85	0.47	0.57	2.11/2.05
4T1BSAc 5% wt	8.60	0.56	0.61	2.92/2.86
4T1BSAc 10% wt	6.48	0.56	0.60	2.18/1.96
4T1BSAc 20% wt	5.34	0.48	0.54	1.39/1.28
4T1B 5%wt	7.97	0.53	0.60	2.54/2.27
4T1B 10% wt	7.98	0.56	0.58	2.59/2.44
4T1B 20% wt	7.88	0.56	0.53	2.37/2.22

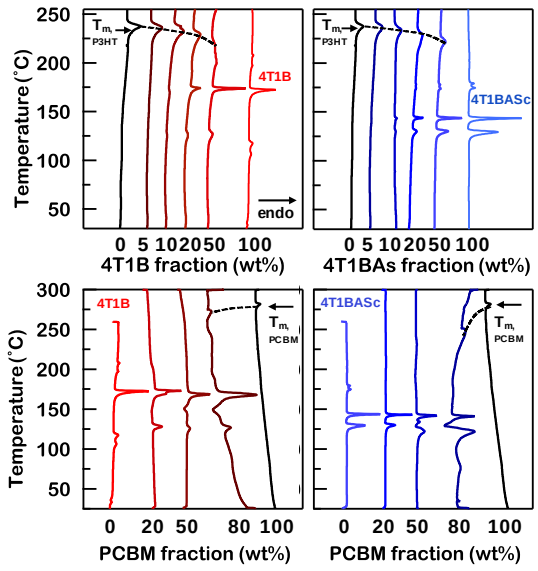

Figure 2. First heating thermograms of a) P3HT:**4T1B**- (left) and P3HT:**4T1BSAc** binary blends (right), and b) for **4T1B**: $PC_{60}BM$- (left) and **4T1BSAc**:$PC_{60}BM$ binary blends (right). The melting point depression of, respectively, P3HT and $PC_{60}BM$ upon mixing with additives is indicated with dotted lines.

slightly improve J_{sc} (**Fig. 1b**; **Table 2**).

The question arises why we observe different device performances in ternaries using the two energy-cascade formers despite they feature very similar energy levels. One possibility is that this is caused by a different phase behavior of the two ternary systems, caused, as expected, by the thiol-functionalization of **4T1BSAc**. We thus conducted DSC measurements focusing on the respective binaries (*i.e.* P3HT:**4T1B**, P3HT:**4T1BSAc**; **4T1B**:$PC_{60}BM$ and **4T1BSAc**:$PC_{60}BM$) rather than the more complex ternaries. This allowed us to assess in a relatively straightforward manner whether one of the additives displays a preferential affinity with the donor or the acceptor material (or both). Thermograms of additive:donor and additive:acceptor binaries are shown in the **Fig. 2**. We observe a similar depression of the melting point of P3HT upon addition of either **4T1B** or **4T1BSAc**, indicating a similar compatibility of P3HT with the two additives. This picture is supported by the relative crystallinity of P3HT, extracted from the DSC data (see SI, Figure S20), that is fairly preserved upon mixing with **4T1B** or **4T1BSAc** at the investigated concentrations. Furthermore, at the highest additive concentration (20% by weight), P3HT shows higher relative crystallinity upon mixing with **4T1BSAc**, suggesting lower miscibility with the thiolated additive. Conversely, the melting point of the fullerene seems notably more depressed when it is blended with **4T1BSAc**, suggesting stronger interactions between this additive and $PC_{60}BM$. In fact, in blends with **4T1B** at 20% content, the presence of a distinct melting endotherm (at 272°C) is characteristic for the presence of residual crystalline PCBM domains. On the contrary, in blends with **4T1BSAc** at 20% content, the endotherm transition originally attributed to PCBM melting transition is shifted of 36°C (from 281 to 245°C), indicating quite probably the formation of a predominant co-crystallized intermixed phase. This view is supported by the fact that we find the additive emission to be stronger quenched in the **4T1BSAc**:$PC_{60}BM$ blends compared to the **4T1B**: $PC_{60}BM$ binaries (see SI, Fig. S14). The presence of the peripheral thioacetyl groups on **4T1BSAc**, structurally related to the aliphatic thiols,[16] justifies the higher miscibility of this small molecule with $PC_{60}BM$.

This higher compatibility seems to be maintained in the ternaries prepared with **4T1BSAc**. In atomic force microscopy (AFM) measurements, we observe – as expected – less aggregates (additive-rich, fullerene-rich, or both) forming in the blends comprising the thiol-functionalised additive, although the surface roughness at higher content of this additive increases compared to systems comprising **4T1B** (Fig. 3). Indeed, the blends with **4T1B** additive, display R_q values of 3.1 ±0.3 nm, 4.2 ±0.8 nm, 3.9 ±0.4 nm for an additive content of 5, 10 and 20 % wt (Fig. 3b, 3c and 3d, respectively), while those comprising **4T1BSAc** feature R_q values of 1.9 ±0.3 nm, 4.4 ±0.8 nm, 5.9 ±0.8 nm for the same additive content (Fig. 3e-g). The intimate mixing produced in **4T1BSAc** additivated blends becomes more evident comparing the 1x1 μm^2 AFM topographies (see SI, Figure S19) of the reference blend and of the same blends with 5% content of additive: while the P3HT:$PC_{60}BM$ reference shows a clear self-segregation attitude, giving origin to regular nanometric aggregates, the blend with **4T1BSAc** shows bigger and regular aggregates suggesting the formation of subnanophases of optimized dimension. In the case of the blend with **4T1B**, the aggregates appear even bigger, probably because of the concurrent lower miscibility of **4T1B** with $PC_{60}BM$ (deduced from the lower depression of the fullerene's melting point observed in DSC upon blending with this additive) and higher compatibility with P3HT (desumed by the higher depression of P3HT's relative crystallinity upon melting with **4T1B**), that enhances phase segregation, promoting formation of polymer-rich bigger domains.

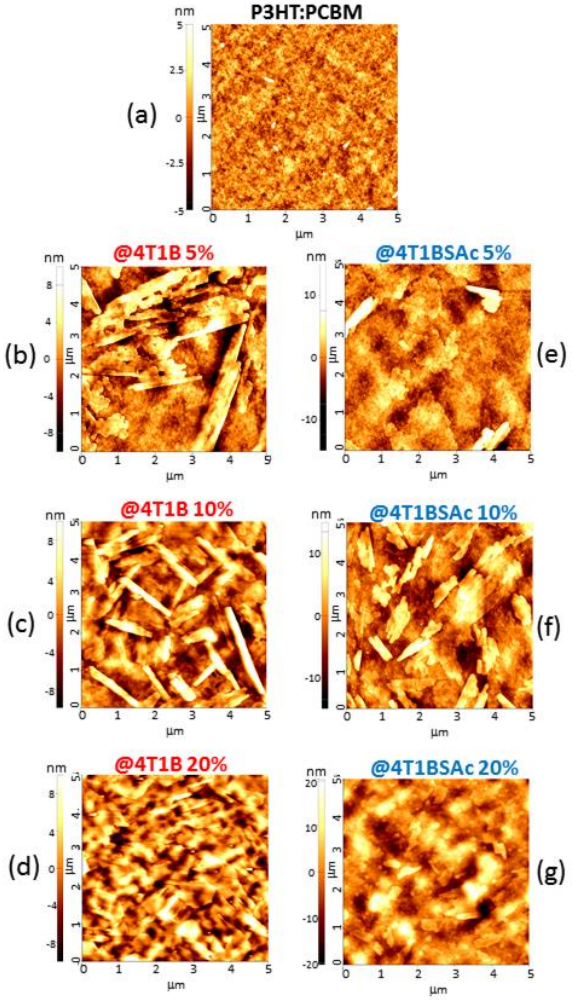

Figure 3. Tapping-mode 5x5 μm^2 AFM topographies of films of P3HT: $PC_{60}BM$ 60:40. a) Without and b-g) with additives (additive contents are indicated in figure).

The formation of bigger aggregates is beneficial for all solar cells, but considering the better performance obtained using **4T1BSAc** additive at 5% content, we must conclude that this blend represents the morphology with the best compromise between

nanophases dimension, intermixed portions and ternary cascade mechanism activation. In other words, when the formation of segregated subnanophases is modulated by the thiolated additive, this allows the formation of small intermixed **4T1BSAc**:$PC_{60}BM$ domains that enhance the ternary cascade activation.

The higher compatibility of **4T1BSAc** with the fullerene derivative seems to be detrimental at higher additive contents. While it may be favorable for creating a close energy cascade, in the case that the additive is too well mixed with the acceptor, electron extraction may be hindered because of insufficient charge transport pathways via fullerene-rich domains. This is further demonstrated by the drop in PCBM relative crystallinity in the binary blend with 20% content of **4T1BSAc** (see Figure 2 and SI, Figure S20). The limited formation of fullerene-rich aggregates is also undesirable for charge generation; aggregates have been shown to be beneficial for exciton dissociation.[22]

Based on our observations, we conclude that when using our additives we can create an energy cascade. To achieve this, their effective miscibility and phase behavior with the donor and acceptor materials play a crucial role and, more specifically, it seems that in the case-in-point, the phase behavior of the additive and fullerene is critical. Clearly further studies are required to elucidate this in detail. What is unambiguous from our data is that both electronic and structural features are important to make ternary systems work providing some information on design criteria for energy cascade additives. Thereby manipulation of the additive's compatibility with either the donor or acceptor material via side chain functionalization appears to be a powerful approach to tune final BHJ structure and finally device performances.

ASSOCIATED CONTENT

Supporting Information

Synthesis, ^{1}H-NMR, ^{13}C-NMR and MALDI-TOF mass spectra, UV-vis absorption and emission spectroscopy, cyclic voltammetry, complete set of DSC data, statistical variations of solar-cell performance, thin-film transistor performance (PDF). The Supporting Information is available free of charge on the ACS Publications website.

AUTHOR INFORMATION

Corresponding Author

gianlucamaria.farinola@uniba.it; natalie.stingelin@mse.gatech.edu

Present Address

° Center for Nano Science and Technology (CNST) of the Istituto Italiano di Tecnologia (IIT), Via Giovanni Pascoli, 70, 20133 Milano, Italy.

Author Contributions

# A.P. and A.O. contributed equally to this work. The manuscript was written by contributions of all authors.

Notes

The authors declare no competing financial interests.

ACKNOWLEDGMENT

This work was financially supported by "XF-actors 727987". AO acknowledges the Regione Puglia for the project "SolarLeaf - (Prot. F6YRA01). The authors thank Miss Cristina Romita for preliminary assistance with the establishement of synthetic procedures and Mr Paolo Guarino for preliminary solar cells experiments. Dr. Maria Michela Giangregorio is gratefully acknowledged for instructing A.O. in the use of AFM.

REFERENCES

1. a) Heeger, A. J. 25th Anniversary Article: Bulk Heterojunction Solar Cells: Understanding the Mechanism of Operation. *Adv. Mater.* **2014**, *26*, 10-28; b) Brabec, C. J.; Gowrishankar, S.; Halls, J. J. M.; Laird, D.; Jia, S.; Williams, S. P. Polymer-fullerene bulk-heterojunction solar cells. *Adv. Mater.* **2010**, *22*, 3839-3856; c) Günes, S.; Neugebauer, H.; Sariciftci, N. S. Conjugated Polymer-Based Organic Solar Cells. *Chem. Rev.* **2007**, *107*, 1324-1338.

2. a) Zhao, W.; Li, S.; Yao, H.; Zhang, S.; Zhang, Y.; Yang, B.; Hou, J. Molecular Optimization Enables over 13% Efficiency in Organic Solar Cells. *J. Am. Chem. Soc.* **2017**, *139*, 7148-7151; b) Zhang, G.; Zhang, K.; Yin, Q.; Jiang, X.-F.; Wang, Z.; Xin, J.; Ma, W.; Yan, H.; Huang, F.; Cao, Y. High-Performance Ternary Organic Solar Cell Enabled by a Thick Active Layer Containing a Liquid Crystalline Small Molecule Donor. *J. Am. Chem. Soc.* **2017**, *139*, 2387-2395; c) Chen, S.; Liu, Y.; Zhang, L.; Chow, P. C. Y.; Wang, Z.; Zhang, G.; Ma, W.; Yan, H. A Wide-Bandgap Donor Polymer for Highly Efficient Non-fullerene Organic Solar Cells with a Small Voltage Loss. *J. Am. Chem. Soc.* **2017**, *139*, 6298-6301.

3. Marzano, G.; Ciasca, C. V.; Bianchi, F.; Pellegrino, A.; Po, R.; Farinola, G. M. Organometallic Approaches to Conjugated Polymers for Plastic Solar Cells: From Laboratory Synthesis to Industrial Production. *Eur. J. Org. Chem.* **2014**, *30*, 6583-6614.

4. Baran, D.; Kirchartz, T.; Wheeler, S.; Dimitrov, S.; Abdelsamie, M.; Gorman, J.; Ashraf, R. S.; Holliday, S.; Wadsworth, A.; Gasparini, N.; Kaienburg, P.; Yan, H.; Amassian, A.; Brabec, C. J.; Durrant, J. R.; McCulloch, I. Reduced voltage losses yield 10% efficient fullerene free organic solar cells with >1 V open circuit voltages. *Energy Environ. Sci.* **2016**, *9*, 3783-3793.

5. a) Ameri, T.; Khoram, P.; Min, J.; Brabec, C. J. Organic Ternary Solar Cells: A Review. *Adv. Mater.* **2013**, *25*, 4245-4266; b) Chen, Y.-C.; Hsu, C.-Y.; Lin, R. Y.-Y.; Ho, K.-C.; Lin, J. T. Materials for the Active Layer of Organic Photovoltaics: Ternary Solar Cell Approach. *ChemSusChem*, **2013**, *6*, 20-35; c) Lu, L.; Kelly, M. A.; You, W.; Yu, L. Status and prospects for ternary organic photovoltaics. *Nature Photonics* **2015**, *9*, 491-500.

6. a) Wang, Y.; Ohkita, H.; Benten, H.; Ito, S. Highly efficient exciton harvesting and charge transport in ternary blend solar cells based on wide- and low-bandgap polymers. *PhysChemChemPhys.*, **2015**, *28*, 27217-27224; b) Lobez, J. M.; Andrew, T. L.; Bulović, V.; Swager, T. M. Improving the performance of P3HT-fullerene solar cells with side-chain-functionalized poly(thiophene) additives: a new paradigm for polymer design. *ACS Nano*, **2012**, *6*, 3044-3056; c) Machui, F.; Rathgeber, S.; Li, N.; Ameri, T.; Brabec, C. J. Influence of a ternary donor material on the morphology of a P3HT:PCBM blend for organic photovoltaic devices. *J. Mater. Chem.* **2012**, *22*, 15570-15577. d) Ameri, T.; Min, J.; Li, N.; Machui, F.; Baran, D.; Forster, M.; Schottler, K. J.; Dolfen, D.; Scherf, U.; Brabec, C. J. Performance Enhancement of the P3HT/PCBM Solar Cells through NIR Sensitization Using a Small-Bandgap Polymer. *Adv. Energy Mater.* **2012**, *2*, 1198-1202.

7. a) Liu, W.; Shi, H.; Fu, W.; Zuo, L.; Wang, L.; Chen, H. Efficient ternary blend polymer solar cells with a bipolar diketopyrrolopyrrole small molecule as cascade material. *Org. Electron.* **2015**, *25*, 219-224; b) Lim, B.; Bloking, J. T.; Ponec, A.; McGehee, M. D.; Sellinger, A. Ternary bulk heterojunction solar cells: addition of soluble NIR dyes for photocurrent generation beyond 800 nm. *ACS Appl. Mater. Interfaces* **2014**, *6*, 6905-6913; c) An, Q.; Zhang, F.; Li, L.; Wang, J.; Zhang, J.; Zhou, L.; Tang, W. Improved efficiency of bulk heterojunction polymer solar cells by doping low-bandgap small molecules. *ACS Appl. Mater. Interfaces* **2014**, *6*, 6537-6544; d) Kokil, A.; Poe, A. M.; Bae, Y.; Della Pelle, A. M.; Homnick, P. J.; Lahti, P. M.; Kumar, J.; Thayumanavan, S. Improved performances in polymer BHJ solar cells through frontier orbital tuning of small molecule additives in ternary blends. *ACS Appl. Mater. Interfaces* **2014**, *6*, 9920-9924; e) Ye, L.; Xia, H.; Xiao, Y.; Xu, J.; Miao, Q. Ternary blend bulk heterojunction photovoltaic cells with an ambipolar small molecule as the cascade material. *RSC Adv.*, **2014**, *4*, 1087-1092; f) Ye, L.; Xu, H.-H.; Yu, H.; Xu, W.-Y.; Li, H.; Wang, H.; Zhao, N.; Xu, J.-B. Ternary Bulk Heterojunction Photovoltaic Cells Composed of Small Molecule Donor Additive as Cascade Material. *J. Phys. Chem. C* **2014**, *118*, 20094-20099; g) Chang, J.-K.; Kuo, Y.-C.; Chen, Y.-J.; Lo, A.-L.; Liu, I-H.; Tseng, W.-H.; Wub, K.-H.; Chen, M.-H.; Wua, C.-I. Bridging donor–acceptor energy offset using organic dopants as energy ladders to improve open-circuit voltages in bulk-heterojunction solar cells. *Org. Electron.* **2014**, *15*, 3458-3464. h) Cha, H.; Chung, D. S.; Bae, S. Y.; Lee, M.-J.; An, T. K.; Hwang, J.; Kim, K. H.; Kim, Y.-H.; Choi, D. H.; Park, C. E. Complementary Absorbing Star-Shaped Small Molecules for the Preparation of Ternary Cascade Energy Structures in Organic Photovoltaic Cells. *Adv. Funct. Mater.* **2013**, *23*, 1556-1565.

8. a) Li, X.; Choy, W.C. H.; Lu, H.; Sha, W. E. I.; Ho, A. H. P. Efficiency Enhancement of Organic Solar Cells by Using Shape-Dependent Broadband Plasmonic Absorption in Metallic Nanoparticles. *Adv. Funct. Mater.* **2013**, *23*, 2728-2735; b) Fu, H.; Choi, M.; Luan, W.; Kim, Y.-S.; Tu, S. T. Hybrid solar cells with an inverted structure: Nanodots incorporated ternary system. *Solid State Electron.* **2012**, *69*, 50-54; c) Wang, D. H.; Kim, D. Y.; Choi, K. W.; Seo, J. H.; Im, S. H.; Park, J. H.; Park, O. O.; Heeger, A. J. Enhancement of donor-acceptor polymer bulk heterojunction solar cell power conversion efficiencies by addition of Au nanoparticles. *Angew. Chem. Int. Ed.* **2011**, *50*, 5519-5523.

9. Melucci, M.; Favaretto, L.; Zanelli, A.; Cavallini, M.; Bongini, A.; Maccagnani, P.; Ostoja, P.; Derue, G.; Lazzaroni, R.; Barbarella, G. Thiophene–Benzothiadiazole Co-Oligomers: Synthesis, Optoelectronic Properties, Electrical Characterization, and Thin-Film Patterning. *Adv. Funct. Mater.* **2010**, *20*, 445-452.

10. Kong, J. A.; Lim, E.; Lee, K. K.; Lee, S.; Kim, S. H. A benzothiadiazole-based oligothiophene for vacuum-deposited organic photovoltaic cells. *Sol. Energy Mater. Sol. Cells* **2010**, *94*, 2057-2063.

11. Sonar, P.; Singh, S. P.; Leclère, P.; Surin, M.; Lazzaroni, R.; Lin, T. T.; Dodabalapur, A.; Sellinger, A. Synthesis, characterization and comparative study of thiophene–benzothiadiazole based donor–acceptor–donor (D–A–D) materials. *J. Mater. Chem.* **2009**, *19*, 3228-3237.

12. Sonar, P.; Singh, S. P.; Sudhakar, S.; Dodabalapur, A.; Sellinger, A. High-Mobility Organic Thin Film Transistors Based on Benzothiadiazole-Sandwiched Dihexylquaterthiophenes. *Chem. Mater.* **2008**, *20*, 3184-3190.

13. Melucci, M.; Favaretto, L.; Bettini, C.; Gazzano, M.; Camaioni, N.; Maccagnani, P.; Ostoja, P.; Monari, M.; Barbarella, G. Liquid-Crystalline Rigid-Core Semiconductor Oligothiophenes: Influence of Molecular Structure on Phase Behaviour and Thin-Film Properties. *Chem. Eur. J.* **2007**, *13*, 10046-10054.

14. a) Punzi, A.; Maiorano, E.; Nicoletta, F.; Blasi, D.; Ardizzone, A.; Ventosa, N.; Ratera, I.; Veciana, J.; Farinola, G. M. 1,2,3-Triazole–Diketopyrrolopyrrole Derivatives with Tunable Solubility and Intermolecular Interactions. *Eur. J. Org. Chem.* **2016**, 2617-2627; b) Punzi, A.; Nicoletta, F.; Marzano, G.; Fortuna, C. G.; Dagar, J.; Brown, T. M.; Farinola, G. M. Synthetic Routes to TEG-Substituted Diketopyrrolopyrrole-Based Low Band-Gap Polymers. *Eur. J. Org. Chem.* **2016**, 3233-3242; c) Punzi, A.; Capozzi, M. A. M.; Fino, V.; Carlucci, C.; Suriano, M.; Mesto, E.; Schingaro, E.; Orgiu, E.; Bonacchi, S.; Leydecker, T.; Samorì, P.; Musio, R.; Farinola, G. M. Croconaines as molecular materials for organic electronics: synthesis, solid state structure and use in transistor devices. *J. Mater. Chem. C* **2016**, *4*, 3138-3142; d) Fiandanese, V.; Marino, I.; Punzi, A. An easy access to 4-(1,2,3-triazolylalkyl)-1,2,3-triazole-fused dihydroisoquinolines and dihydroisoindoles. *Tetrahedron* **2012**, *68*, 10310-10317; e) Operamolla, A.; Colella, S.; Musio, R.; Loiudice, A.; Hassan Omar, O.; Melcarne, G.; Mazzeo, M.; Gigli, G.; Farinola, G. M.; Babudri, F. Low band gap poly(1,4-arylene-2,5-thienylene)s with benzothiadiazole units: Synthesis, characterization and application in polymer solar cells. *Sol. Energy Mater. Sol. Cells* **2011**, *95*, 3490-3503; f) Hassan Omar, O.; Babudri, F.; Farinola, G. M.; Naso, F.; Operamolla, A.; Pedone, A. Synthesis of D-glucose and L-phenylalanine substituted phenylene-thiophene oligomers. *Tetrahedron* **2011**, *67*, 486-494; g) Hassan Omar, O.; la Gatta, S.; Tangorra, R. R.; Milano, F.; Ragni, R.; Operamolla, A.; Argazzi, R.; Chiorboli, C.; Agostiano, A.; Trotta, M.; Farinola, G. M. Synthetic Antenna Functioning As Light Harvester in the Whole Visible Regio for Enhanced Hybrid Photosynthetic Reaction Centers. *Bioconj. Chem.* **2016**, *27*, 1614-1623; h) Sgobba, V.; Giancane, G.; Cannoletta, D.; Operamolla, A.; Hassan Omar, O.; Farinola, G. M.; Guldi, D. M.; Valli, L. Langmuir−Schaefer Films for Aligned Carbon Nanotubes Functionalized with a Conjugated Polymer and Photoelectrochemical Response Enhancement *ACS Appl. Mater. Interfaces* **2014**, *6*, 153-158.

15. Operamolla, A.; Punzi, A.; Farinola, G. M. Synthetic Routes to Thiol Functionalized Organic Semiconductors for Molecular and Organic Electronics. *Asian J. Org. Chem.* **2017**, *6*, 120-138.

16. a) Lee, J. K.; Ma, W. L.; Brabec, C. J.; Yuen, J.; Moon, J. S.; Kim, J. Y.; Lee, K.; Bazan, G. C.; Heeger, A. J. Processing Additives for Improved Efficiency from Bulk Heterojunction Solar Cells. *J. Am. Chem. Soc.* **2008**, *130*, 3619-3623; b) Pivrikas, A.; Stadler, P.; Neugebauer, H.; Sariciftci, N. S. Substituting the postproduction treatment for bulk-heterojunction solar cells using chemical additives. *Org. Electron.* **2008**, *9*, 775-782; c) Yao, Y.; Hou, J.; Xu, Z.; Li, G.; Yang, Y. Effects of Solvent Mixtures on the Nanoscale Phase Separation in Polymer Solar Cells. *Adv. Funct. Mater.* **2008**, *18*, 1783-1789.

17. a) Honda, S.; Ohkita, H.; Benten, H.; Ito, S. Selective Dye Loading at the Heterojunction in Polymer/Fullerene Solar Cells. *Adv. Energy Mater.* **2011,** *1*, 588-598; b) Honda, S.; Nogami, T.; Ohkita, H.; Benten, H.; Ito, S. Improvement of the Light-Harvesting Efficiency in Polymer/Fullerene Bulk Heterojunction Solar Cells by Interfacial Dye Modification. *ACS Appl. Mater. Interfaces*, **2009**, *1*, 804-810.

18.a) Jeanbourquin, X. A.; Rahmanudin, A.; Yu, X.; Johnson, M.; Guijarro, N.; Yao, L.; Sivula, K. Amorphous Ternary Charge-Cascade Molecules for Bulk Heterojunction Photovoltaics. *ACS Appl. Mater. Interfaces*, **2017**, *9*, 27825-27831; b) Tan, W-Y.; Gao, K.; Zhang, J.; Chen, L-L.; Wu, S-P;. Jiang, X-F; Peng, X-B.; Hu, Q.; Liu, F.; Wu, H-B.; Cao, Y.; Zhu, X-H. Enhancing Performances of Solution-Processed Inverted Ternary Small-Molecule Organic Solar Cells: Manipulating the Host-Guest Donors and Acceptor Interaction. *Sol. RRL* **2017**, *1*, 1600003; c) Su, W.; Fan, Q.; Guo, X.; Guo, B.; Li, W.; Zhang, Y.; Zhang, M.; Li, Y. Efficient ternary blend all-polymer solar cells with a polythiophene derivative as a hole-cascade material. *J. Mater. Chem. A*, **2016**, *4*, 14752-14760.

19. Cardona, C. M.; Li, W.; Kaifer, A. E.; Stockdale, D.; Bazan, G. C. Electrochemical Considerations for Determining Absolute Frontier Orbital Energy Levels of Conjugated Polymers for Solar Cell Applications. *Adv. Mater.* **2011**, *23*, 2367.

20. a) Lu, L.; Xu, T.; Chen, W.; Landry, E. S.; Yu, L. Ternary blend polymer solar cells with enhanced power conversion efficiency. *Nature Photon.* **2014**, *8*, 716–722. b) Khlyabich, P. P.; Rudenko, A. E.; Street, R. A.; Thompson, B. C. Influence of Polymer Compatibility on the Open-Circuit Voltage in Ternary Blend Bulk Heterojunction Solar Cells. *ACS Appl. Mater. Interfaces.* **2014**, *6*, 9913-9919.

21. a) Khlyabich, P. P.; Burkhart, B.; Thompson, B. C. Compositional Dependence of the Open-Circuit Voltage in Ternary Blend Bulk Heterojunction Solar Cells Based on Two Donor Polymers. *J. Am. Chem. Soc.* **2012**, 134, 9074-9077; b) Street, R. A.; Davies, D.; Khlyabich, P. P.; Burkhart, B.; Thompson, B. C. Origin of the Tunable Open-Circuit Voltage in Ternary Blend Bulk Heterojunction Organic Solar Cells. *J. Am. Chem. Soc.* **2013,** *135*, 986-989.

22. a) Jamieson, F. C.; Buchaca Domingo, E.; McCarthy-Ward, T.; Heeney, M.; Stingelin, N.; Durrant, J. R. Fullerene crystallisation as a key driver of charge separation in polymer/fullerene bulk heterojunction solar cells. *Chem. Sci.* **2012**, *3*, 485-492; b) Buchaca-Domingo, E.; Ferguson, A. J.; Jamieson, F. C.; McCarthy-Ward, T.; Shoaee, S.; Tumbleston, J. R.; Reid, O. G.; Yu, L.; Madec, M.-B.; Pfannmöller, M.; Hermerschmidt, F.; Schröder, R. R.; Watkins, S. E.; Kopidakis, N.; Portale, G.; Amassian, A.; Heeney, M.; Ade, H.; Rumbles, G.; Durrant, J. R.; Stingelin, N. Additive-assisted supramolecular manipulation of polymer:fullerene blend phase morphologies and its influence on photophysical processes. *Mater. Horiz.* **2014**, *1*, 270-279.

Authors are required to submit a graphic entry for the Table of Contents (TOC) that, in conjunction with the manuscript title, should give the reader a representative idea of one of the following: A key structure, reaction, equation, concept, or theorem, etc., that is discussed in the manuscript. Consult the journal's Instructions for Authors for TOC graphic specifications.

Insert Table of Contents artwork here